BELLEFONTE SPENT FUEL STORAGE RACK

LICENSING REPORT

May 22, 1981

WESTINGHOUSE ELECTRIC CORPORATION
Nuclear Energy Systems
P. O. Box 355
Pittsburgh, Pennsylvania 15230

1. INTRODUCTION

This report provides a description of the spent fuel storage racks for the Bellefonte Nuclear Power Plant and the technical information necessary for evaluating the safety aspects of these racks.

2. DESCRIPTION OF RACKS

2.1 GENERAL DESCRIPTION

The function of the spent fuel storage racks is to provide for storage of the maximum possible number of new or spent fuel assemblies in flooded pools, while maintaining a coolable geometry, preventing criticality, and protecting the fuel assemblies from excess mechanical or thermal loadings. The fuel storage rack is composed of individual storage cells. Each cell has a lead-in opening which is symmetrical and is blended smooth. This opening precludes insertion of the fuel assemblies in other than the prescribed locations. The cells are interconnected to form an integral structure. The integral modules are provided with lateral seismic restraint by shear pins and adapter plates. The adapter plates are bolted to embedment studs which are anchored to the floor of the spent fuel pool. Each rack module is provided with leveling pads which are remotely adjustable from above through the cells at installation.

The data listed below is typical for both Units 1 and 2.

Number of Cells	1058
Number Rack Arrays	2 - 11 x 11 4 - 11 x 12 2 - 12 x 12
Poison Material	Boral, .02 gm $^{10}B/cm^2$ Sealed from pool environment.

Center-to-Center Spacing	10.50 in.
Type of Fuel	B&W 17 x 17, 3.6 weight percent enrichment
Seismic Restraints	Adapter plates with shear pins bolted to embedment studs.
Rack Assembly Dimension & Weights	11 x 11 - 116 x 116 x 176 - 31,400 lbs. 11 x 12 - 116 x 126 x 176 - 34,200 lbs. 12 x 12 - 126 x 126 x 176 - 37,300 lbs.

The pool floor embedments and the rack arrangements are shown in Figures 2-1 and 2.2.

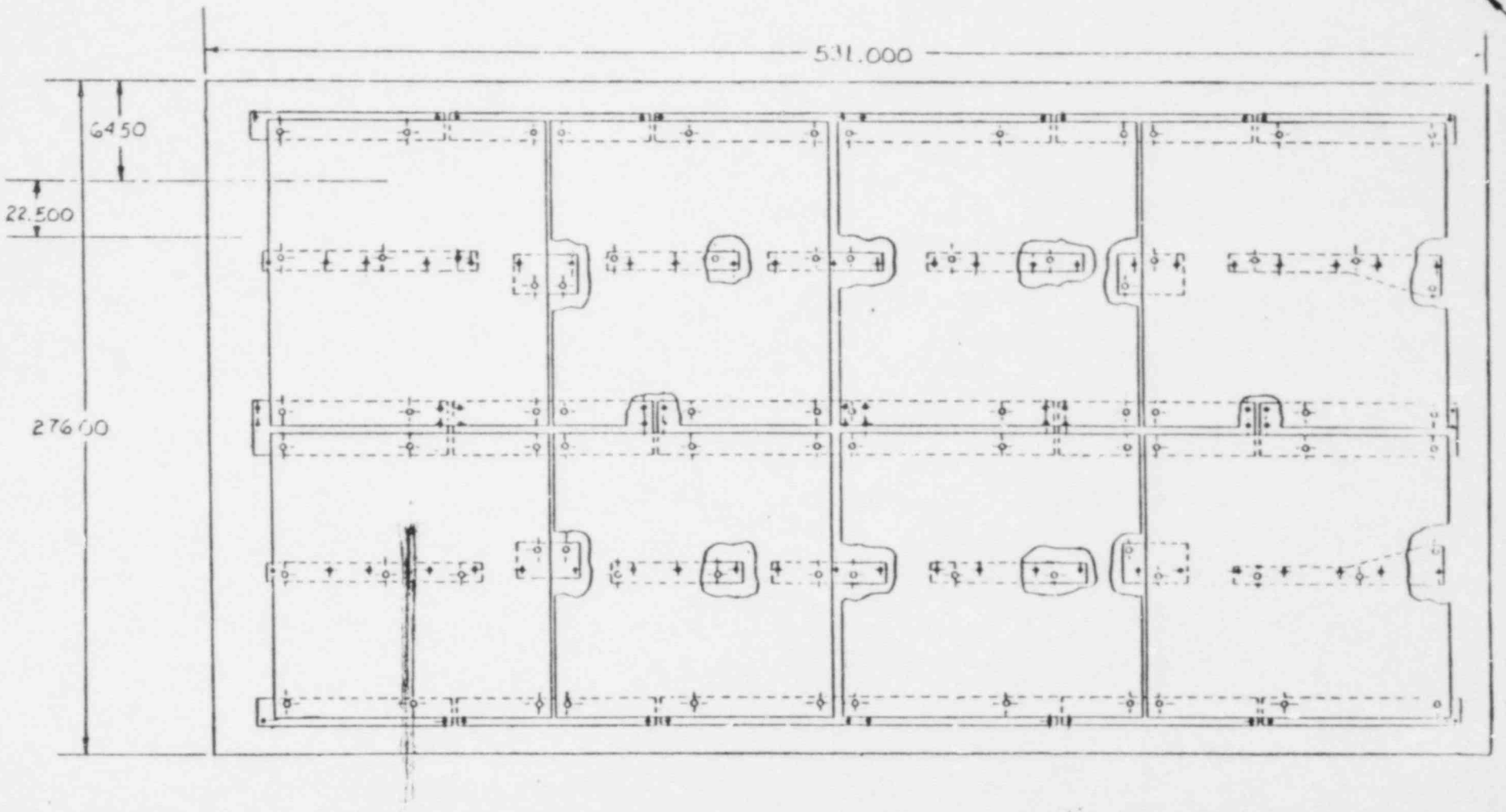

FIGURE 2-1

POOL FLOOR EMBEDMENT OUTLINE

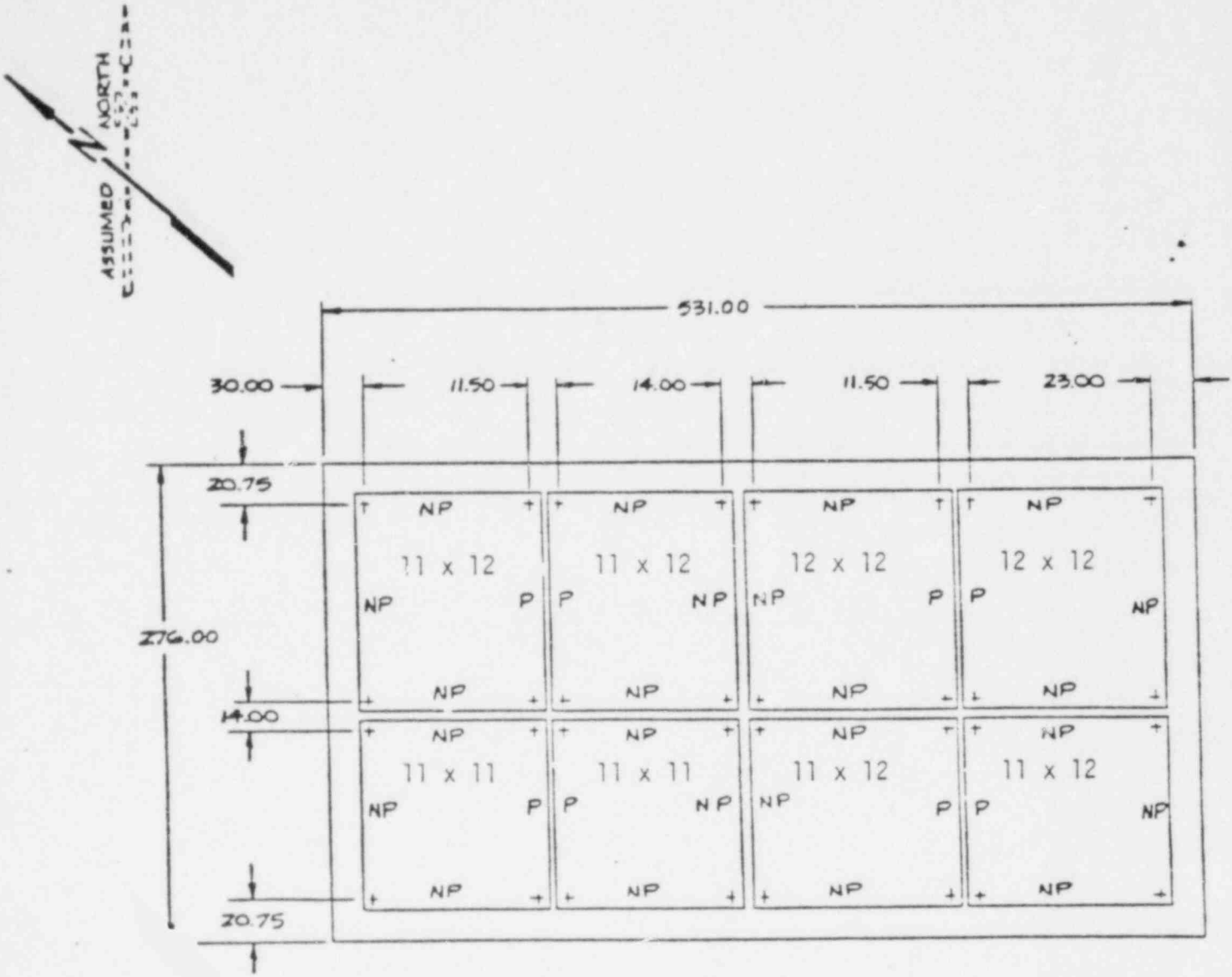

POISON ARRANGEMENT

P = Peripheral Poison
NP = No Peripheral Poison

FIGURE 2-2

GENERAL ARRANGEMENT OF RACKS IN THE POOL

2.2 DESIGN BASES

A list of design criteria is given below:

a. The racks are designed in accordance with the "NRC Position for Review and Acceptance of Spent Fuel Storage and Handling Applications," dated April 14, 1978 and revised January 18, 1979.

b. The racks are designed to meet the nuclear requirements of ANSI N210-1976. The effective multiplication factor, K_{eff}, in the spent fuel pool is less than or equal to 0.95, including all uncertainties and under all credible conditions as described in Section 3.

c. The racks are designed to allow coolant flow such that boiling in the water channels between the fuel assemblies in the rack does not occur. Maximum fuel cladding temperatures are calculated for various pool cooling conditions as described in Section 4.4.

d. The racks are designed to Seismic Category I requirements, and are classified as ANS Safety Class 3 and ASME Code Class 3 Component Support structures. The structural evaluation and seismic analyses are performed using the specified loads and load combinations given in Section 2.3.

e. The racks are designed to withstand loads which may result from fuel handling accidents and from the maximum uplift force of the fuel handling crane.

f. Each storage position in the racks is designed to support and guide the fuel assembly in a manner that will minimize the possibility of application of excessive lateral, axial and bending loads to fuel assemblies during fuel assembly handling and storage.

g. The racks are designed to preclude the insertion of a fuel assembly in other than design locations.

h. The materials used in construction of the racks are compatible with the storage pool environment and do not contaminate the fuel assemblies.

2.3 SPECIFIED LOADS AND DEFINITIONS

The following are load combinations specified for racks:

Elastic Analysis	Acceptance Limits
(1) D +L	Normal Limits of NF 3231.1a
(2) D + L + E	Normal Limits of NF 3231.1a
(3) D + L + T_o	Lesser of 2 S_y or S_u Stress Range
(4) D + L + T_o + E	Lesser of 2 2_y or S_u Stress Range
(5) D + L + T_a + E	Lesser of 2 S_y or S_u Stress Range
(6) D + L + T_a + E'	Faulted Condition Limits of NF 3231.1c

Definitions:

D - Dead loads or their related internal moments and forces including any permanent equipment and hydrostatic loads.

L - Live loads or their related internal moments and forces including any movable equipment loads.

T_o - Thermal effects and loads during normal operating or shutdown conditions, based on the most critical transient or steady-state condition.

T_a - Highest temperature associated with the postulated abnormal design condition.

E - Loads generated by the operating basis earthquake.

E' - Loads generated by the safe shutdown earthquake.

Analyses were performed to verify the acceptability of the critical load components and paths under the load combinations given above.

2.4 DESIGN LOADS

D - Weight of 11 x 11 rack dry . . . . . 31,400 lbs.
Weight of 11 x 12 rack dry . . . . . 34,200 lbs.
Weight of 12 x 12 rack dry ..... 37,200 lbs.

L - Live loads are negligible since the fuel assemblies are lowered very slowly into the cells.

T_o - Service expansion temperature range $\Delta T = 20^{\circ}F$.

T_a - A postulated design condition that would cause T_a is failure of the spent fuel pool cooling system. The water will gradually heat up and boiling could theoretically occur; however, since this process is slow, it is predicted to remain in the T_o ΔT range.

E - Embedment loads per seismic restraint for OBE

E' - Embedment loads per seismic restraint for SSE

2.5 APPLICABLE CODES AND STANDARDS

"NRC Position for Review and Acceptance of Spent Fuel Storage and Handling Applications" dated April 14, 1978 and revised January 18, 1979.

NRC Regulatory Guides

R.G. 1.13 Spent Fuel Storage Facility Design Basis

R.G. 1.29 Seismic Design Classifications

R.G. 1.60 Design Response Spectra for Seismic Design of Nuclear Power Plants

R.G. 1.61 Damping Values for Seismic Design of Nuclear Power Plants

R.G. 1.92 Combining Modal Responses and Spatial Components in Seismic Response Analysis

R.G. 1.124 Service Limits and Loading Combinations for Class I Linear Type Component Supports

NRC Standard Review Plans

SRP 3.7 Seismic Design

SRP 3.8.4 Other Category I Structures

SRP 9.1.2 Spent Fuel Storage

SRP 9.1.3 Spent Fuel Pool Cooling and Cleanup System

Industry Codes and Standards

American Society of Mechanical Engineers, Boiler and Pressure Vessel Code, Section III, Division 1.

American National Standards Institute, N210-1976, "Design Objectives for Light Water Reactor Spent Fuel Storage Facilities at Nuclear Power Stations."

American National Standards Institute, N16.1-1975, "Nuclear Criticality Safety in Operations with Fissionable Materials Outside Reactors."

3. NUCLEAR CONSIDERATIONS

3.1 NEUTRON MULTIPLICATION FACTOR

Criticality of fuel assemblies in the spent fuel storage rack is prevented by the design of the rack which limits fuel assembly interaction. This is done by fixing the minimum separation between assemblies and inserting neutron poisons between assemblies.

The design basis for preventing criticality outside the reactor is that, including uncertainties, there is a 95 percent probability at a 95 percent confidence level that the effective multiplication factor (K_{eff}) of the fuel assembly array will be less than 0.95 as recommended in ANSI N210-1976 and in "NRC Position for Review and Acceptance of Spent Fuel Storage and Handling Applications."

The following are the conditions that are assumed in meeting this design basis.

3.2 NORMAL STORAGE

a. The fuel assembly contains the highest enrichment authorized without any control rods or any noncontained burnable poison and is at its most reactive point in life. The enrichment of the fuel assembly is 3.6 w/o U-235 with no depletion or fission product buildup.

b. The moderator is pure water at the temperature within the design limits of the pool which yields the largest reactivity. A conservative value of 1.0 gm/cm^3 is used for the density of water. No dissolved boron is included in the water.

c. The array is either infinite in lateral extent or is surrounded by a conservatively chosen reflector, whichever is appropriate for the design. The nominal case calculation is infinite in lateral and axial extent. However, poison plates are not

necessary on the periphery of the rack and on one side of the long axis between modules because calculations show that this finite rack is less reactive than the nominal case infinite rack. Therefore, the nominal case of an infinite array of poison cells is a conservative assumption.

d. Mechanical uncertainties and biases due to mechanical tolerances during construction are treated by either using "worst case" conditions or by performing sensitivity studies and obtaining appropriate values. The items included in the analysis are:

- Poison thickness
- Stainless steel thickness
- Can ID
- Center-to-center spacing

The calculational method uncertainty and bias is discussed in Section 3.4.

e. Credit is taken for the neutron absorption in full length structural materials and in solid materials added specifically for neutron absorption. A minimum poison loading is assumed in the poison plates.

3.3 POSTULATED ACCIDENTS

Most accident conditions will not result in an increase in K_{eff} of the rack. Examples are the loss of cooling systems (reactivity decreases with decreasing water density) and dropping a fuel assembly on top of the rack (the rack structure pertinent for criticality is not deformed and the dropped assembly has more than eight inches of water separating it from the rest of the rack which precludes interaction).

However, accidents can be postulated which would increase reactivity. Therefore, for accident conditions, the double contingency principle of ANS N16.1-1975 is applied. This states that it shall require two

unlikely, independent, concurrent events to produce a criticality accident. Thus, for accident conditions, the presence of soluble boron in the storage pool water is assumed as a realistic initial condition.

The presence of approximately 2000 ppm boron in the pool water will decrease reactivity by about 30 percent Δk. In perspective, this is more negative reactivity than is present in the poison plates, so K_{eff} for the rack would be less than 0.95 even if the poison plates were not present. Thus, $K_{eff} < 0.95$ can be easily met for postulated accidents, since any reactivity increase will be much less than the negative reactivity worth of the dissolved boron.

For fuel storage applications, water is usually present. However, accidental criticality when fuel assemblies are stored in the dry conditions is also accounted for. For this case, possible sources of moderation, such as those that could arise during fire fighting operations, are included in the analysis.

This "optimum moderation" accident is not a problem in spent fuel storage racks because possible water densities are too low (< 0.01 gm/cm^3) to yield K_{eff} values higher than for full density water and the rack design prevents the preferential reduction of water density between the cells of a rack (e.g., boiling between cells). Further, the presence of poison plates removes the conditions necessary for "optimum moderation" so that K_{eff} continually decreases as moderator density decreases from 1.0 gm/cm^3 to 0.0 gm/cm^3 in poison rack designs.

3.4 CRITICALITY ANALYSIS

The calculation method and cross-section values are verified by comparison with critical experiment data for assemblies similar to those for which the racks are designed. This benchmarking data is sufficiently diverse to establish that the method bias and uncertainty will apply to rack conditions which include strong neutron absorbers, large water gaps and low moderator densities.

The design method which insures the criticality safety of fuel assemblies in the spent fuel storage rack uses the AMPX system of codes[1,2] for cross-section generation and KENO IV[3] for reactivity determination.

The 218 energy group cross-section library[1] that is the common starting point for all cross-sections used for the benchmarks and the storage rack is generated from ENDF/B-IV data. The NITAWL program[2] includes, in this library, the self-shielded resonance cross-sections that are appropriate for each particular geometry. The Nordheim Integral Treatment is used. Energy and spatial weighting of cross-sections is performed by the XSDRNPM program[2] which is a one-dimensional S_N transport theory code. These multi-group cross-section sets are then used as input to KENO IV[3] which is a three-dimensional Monte Carlo theory program designed for reactivity calculations.

A set of 27 critical experiments has been analyzed using the above method to demonstrate its applicability to criticality analysis and to establish the method bias and variability. The experiments range from water moderated, oxide fuel arrays separated by various materials (Boral, steel, water) that simulate LWR fuel shipping and storage conditions[4,5] to dry, harder spectrum uranium metal cylinder arrays with various interspersed materials[6] (Plexiglas, steel and air) that demonstrate the wide range of applicability of the method.

The results and some descriptive facts about each of the 27 benchmark critical experiments are given in Table 3-1.

The average K_{eff} of the benchmarks is 0.9998 which demonstrates that there is no bias associated with the method. The standard deviation of the K_{eff} values is 0.0057 Δk. The 95/95 one sided tolerance limit factor for 27 values is 2.26. Thus, there is a 95 percent probability with a 95 percent confidence level that the uncertainty in reactivity, due to the method, is not greater than 0.013 Δk.

TABLE 3-1

BENCHMARK CRITICAL EXPERIMENTS [4,5,6]

	General Description	Enrichment w/o U235	Reflector	Separating Material	Characterizing Separation (cm)	K_{eff}
1.	UO_2 rod lattice	2.35	water	water	11.92	1.004 ± .004
2.	"	"	"	"	8.39	0.993 ± .004
3.	"	"	"	"	6.39	1.005 ± .004
4.	"	"	"	"	4.46	0.994 ± .004
5.	"	"	"	stainless steel	10.44	1.005 ± .004
6.	"	"	"	"	11.47	0.992 ± .004
7.	"	"	"	"	7.76	0.992 ± .004
8.	"	"	"	"	7.42	1.004 ± .004
9.	"	"	"	boral	6.34	1.005 ± .004
10.	"	"	"	"	9.03	0.992 ± .004
11.	"	"	"	"	5.05	1.001 ± .004
12.	"	4.29	"	water	10.64	0.999 ± .005
13.	"	"	"	stainless steel	9.76	0.999 ± .005
14.	"	"	"	"	8.08	0.998 ± .006
15.	"	"	"	boral	6.72	0.998 ± .005
16.	U metal cylinders	93.2	bare	air	15.43	0.988 ± .003
17.	"	"	paraffin	air	23.84	1.006 ± .005
18.	"	"	bare	air	19.97	1.005 ± .003
19.	"	"	paraffin	air	36.47	1.001 ± .004
20.	"	"	bare	air	13.74	1.005 ± .003
21.	"	"	paraffin	air	23.48	1.005 ± .004
22.	"	"	bare	plexiglas	15.74	1.010 ± .003
23.	"	"	paraffin	plexiglas	24.43	1.006 ± .004
24.	"	"	bare	plexiglas	21.74	0.999 ± .003
25.	"	"	paraffin	plexiglas	27.94	0.994 ± .005
26.	"	"	bare	steel	14.74	1.000 ± .003
27.	"	"	bare	plexiglas, steel	16.67	0.996 ± .003

The total uncertainty to be added to a criticality calculation is:

$$TU = [(KS)^2_{method} + (KS)^2_{nominal}]^{1/2}$$

where $(KS)_{method}$ is 0.013 as discussed above and $(KS)_{nominal}$ is the statistical uncertainty associated with the particular KENO calculation being used.

The criticality design criteria are met when the calculated effective multiplication factor, plus the total uncertainty (TU) and any biases, is less than 0.95.

These methods conform with ANSI N18.2-1973, "Nuclear Safety Criteria for the Design of Stationary Pressurizer Water Reactor Plants," Section 5.7, Fuel Handling System; ANSI N210-1976, "Design Objectives for LWR Spent Fuel Storage Facilities at Nuclear Power Stations," Section 5.1.12; ANSI N16.9-1975, "Validation of Calculational Methods for Nuclear Criticality Safety," NRC Standard Review Plan, Section 9.1.2, "Spent Fuel Storage"; and the NRC guidance, "NRC Position for Review and Acceptance of Spent Fuel Storage and Handling Applications."

3.5 RACK MODIFICATION

The spent fuel storage rack is described in Section 2.0. The minimum ^{10}B loading in the poison plates is 0.02 gm $^{10}B/cm^2$.

For normal operation and using the method in the above sections, the K_{eff} for the rack is determined in the following manner.

$$K_{eff} = K_{nominal} + B_{mech} + B_{method} + B_{part} + [(KS_{nominal})^2 + (KS_{method})^2]^{1/2}$$

where:

$K_{nominal}$ = nominal case KENO K_{eff}

B_{mech} = K_{eff} bias to account for the fact that mechanical tolerances can result in water gaps between poison plates less than nominal.

B_{method} = method bias determined from benchmark critical comparisons.

B_{part} = bias to account for poison particle self-shielding.

$KS_{nominal}$ = 95/95 uncertainty in the nominal case KENO K_{eff}.

KS_{method} = 95/95 uncertainty in the method bias.

Substituting calculated values, the result is:

K_{eff} = 0.9474

Since K_{eff} is less than 0.95 including uncertainties at a 95/95 probability/confidence level, the acceptance criteria for criticality is met.

3.6 ACCEPTANCE CRITERIA FOR CRITICALITY

The neutron multiplication factor in spent fuel pools shall be less than or equal to 0.95, including all uncertainties, under all conditions.

Generally, the acceptance criteria for postulated accident conditions can be $K_{eff} \leq 0.98$ because of the accuracy of the methods used coupled with the low probability of occurrence. For instance, in ANSI N210-1976 the acceptance criteria for the "optimum moderation" condition is $K_{eff} \leq 0.98$. However, for storage pools, which contain dissolved boron, the use of the realistic initial conditions ensures that $K_{eff} << 0.95$ for postulated accidents as discussed in Section 2.3.2.3. Thus, for simplicity the acceptance criteria for all conditions will be $K_{eff} \leq .95$.

4. THERMAL AND HYDRAULIC CONSIDERATIONS

The purpose of thermal-hydraulic analysis is to determine the maximum fuel clad temperatures which may occur as a result of using the poison spent fuel racks in the Bellefonte spent fuel pool.

4.1 CRITERIA

The criteria used to determine the acceptability of the design from a thermal-hydraulic viewpoint have been taken from References 7 through 10. Briefly stated, the criteria may be summarized as follows.

a. The design must allow adequate cooling by natural circulation and by flow provided by spent fuel pool cooling system. The coolant should remain subcooled at all points within the pool when the cooling system is operational. When the cooling system is postulated to be inoperable, adequate cooling implies that the temperature of the fuel cladding should be sufficiently low that no structural failures would occur and that no safety concerns would exist.

b. For normal operations, the maximum pool temperature shall not exceed 150°F. For conservatism, the temperatures of the storage racks and the stored fuel are evaluated assuming that the temperature of the water at the inlet to the storage cells is 150°F during normal operation.

c. The rack design must not allow trapped air or steam and direct gamma heating of the storage cell walls and the intercell water must be considered.

4.2 KEY ASSUMPTIONS

a. The nominal water level is 24 feet above the top of the fuel storage racks.

b. The maximum fuel assembly decay heat output is 63.4 Btu/sec. which is based on the fuel characteristics given in Attachment No. 5 to Reference 7 and corresponds to 150 hours after shutdown.

c. The maximum temperature of the water at the inlet to the storage cells is 150°F when the cooling system is operational.

d. Under postulated accident conditions, when no pool cooling systems are operational, the maximum temperature at the inlet to the cells is assumed to be equal to the saturation temperature at atmospheric pressure or 212°F.

4.3 DESCRIPTION OF ANALYTICAL METHOD AND TYPES OF CALCULATIONS PERFORMED

A natural circulation calculation is employed to determine the thermo-hydraulic conditions within the spent fuel storage cells. The model used assumes that all downflow occurs in the peripheral gap between the pool walls and the outermost storage cells and all lateral flow occurs in the space between the bottom of the racks and the bottom of the pool. The effect of flow area blockage in the region is conservatively accounted for and a multi-channel formulation is used to determine the variation in axial flow velocities through the various storage cells. The hydraulic resistance of the storage cells and the fuel assemblies is conservatively modelled by applying large uncertainty factors to loss coefficients obtained from various sources. Where necessary, the effect of Reynolds Number on the hydraulic resistance is considered and the variation in momentum and elevation head pressure drops with fluid density is also determined.

The solution is obtained by iteratively solving the conservation equations (mass, momentum and energy) for the natural circulation loops and the flow velocities and fluid temperatures that are obtained are then used to determine the fuel cladding temperatures. An elevation view of

a typical model is sketched in Figure 4-1 where the flow paths are indicated by arrows. Note that each cell shown in that sketch actually corresponds to a row of cells that are located at the same distance from the pool walls. This is more clearly shown in a plan view, Figure 4-2.

As shown in that sketch, the lateral flow area underneath the storage cells decreases as the distance from the wall increases. This counteracts the decrease in the total lateral flow that occurs because of flow that branches up and flows into the cells. This is significant because the lateral flow velocity affects both the lateral pressure drop underneath the cells and the turning losses that are experienced as the flow branches up into the cells. These effects are considered in the natural circulation analysis.

The most recently discharged or "hottest" fuel assemblies are assumed to be located in various rows during different calculations in order to ensure that they may be placed anywhere within the pool without violating safety limits. In order to simplify the calculations, each row of the model must be composed of storage cells having a uniform decay heat level. This decay heat level may or may not correspond to a specific batch of fuel, but the model is constructed so that the total heat input is correct. The "hottest" fuel assemblies are all assumed to be placed in a given row of the model in order to ensure that conservatively accurate results are obtained for those assemblies.

Since the natural circulation velocity strongly affects the temperature rise of the water and the heat transfer coefficient within a storage cell, the hydraulic resistance experienced by the flow is a significant parameter in the evaluation. In order to minimize the resistance, the design of the inlet region of the racks has been chosen such as to maximize this flow area. Each storage cell has at least three separate flow openings as shown in Figure 4-3. The use of these multiple flow holes virtually eliminates the possibility that all flow into the inlet of a given cell can be blocked by debris or other foreign material that may get into the pool.

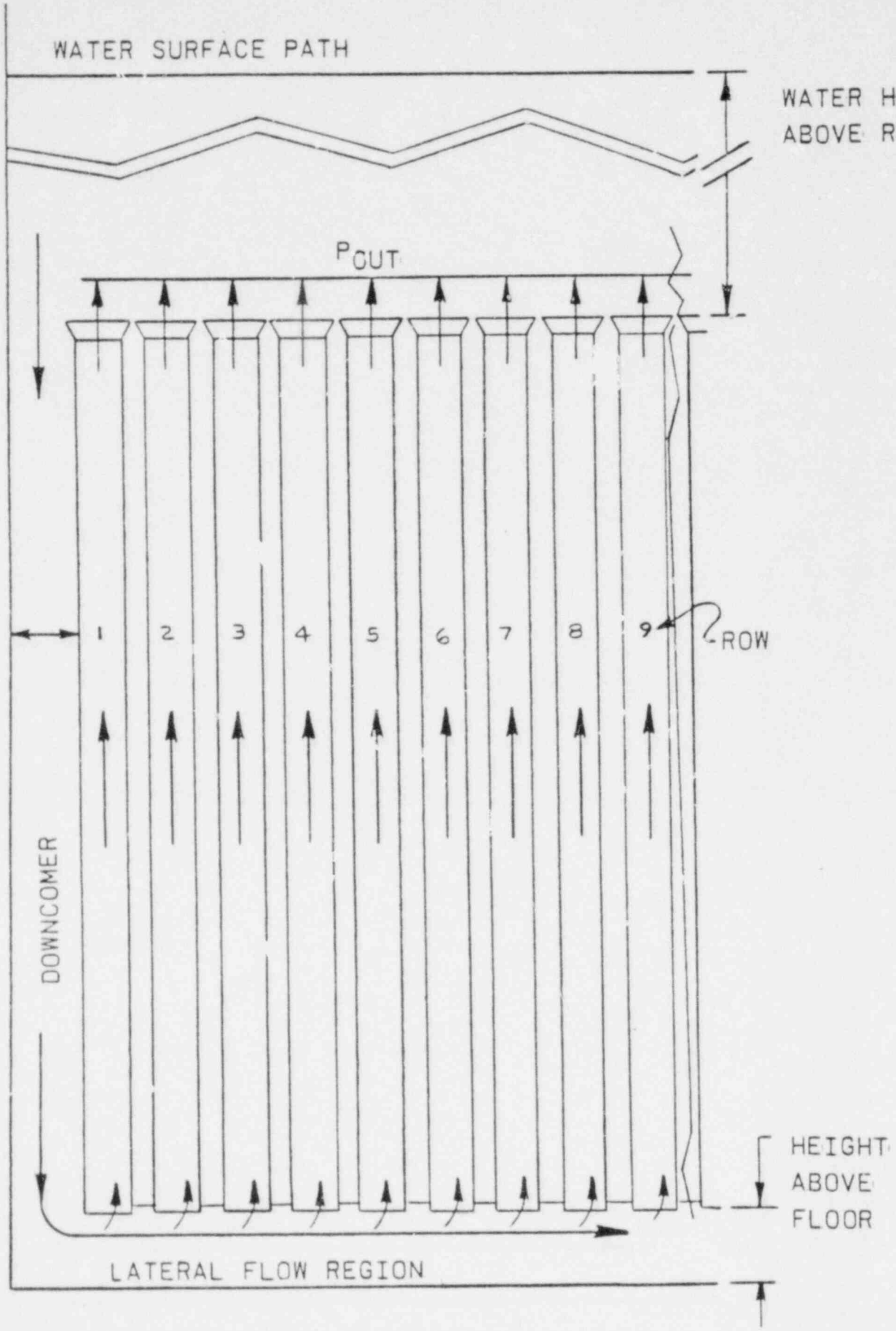

FIGURE 4-1

SPENT FUEL POOL NATURAL CIRCULATION MODEL

(ELEVATION VIEW)

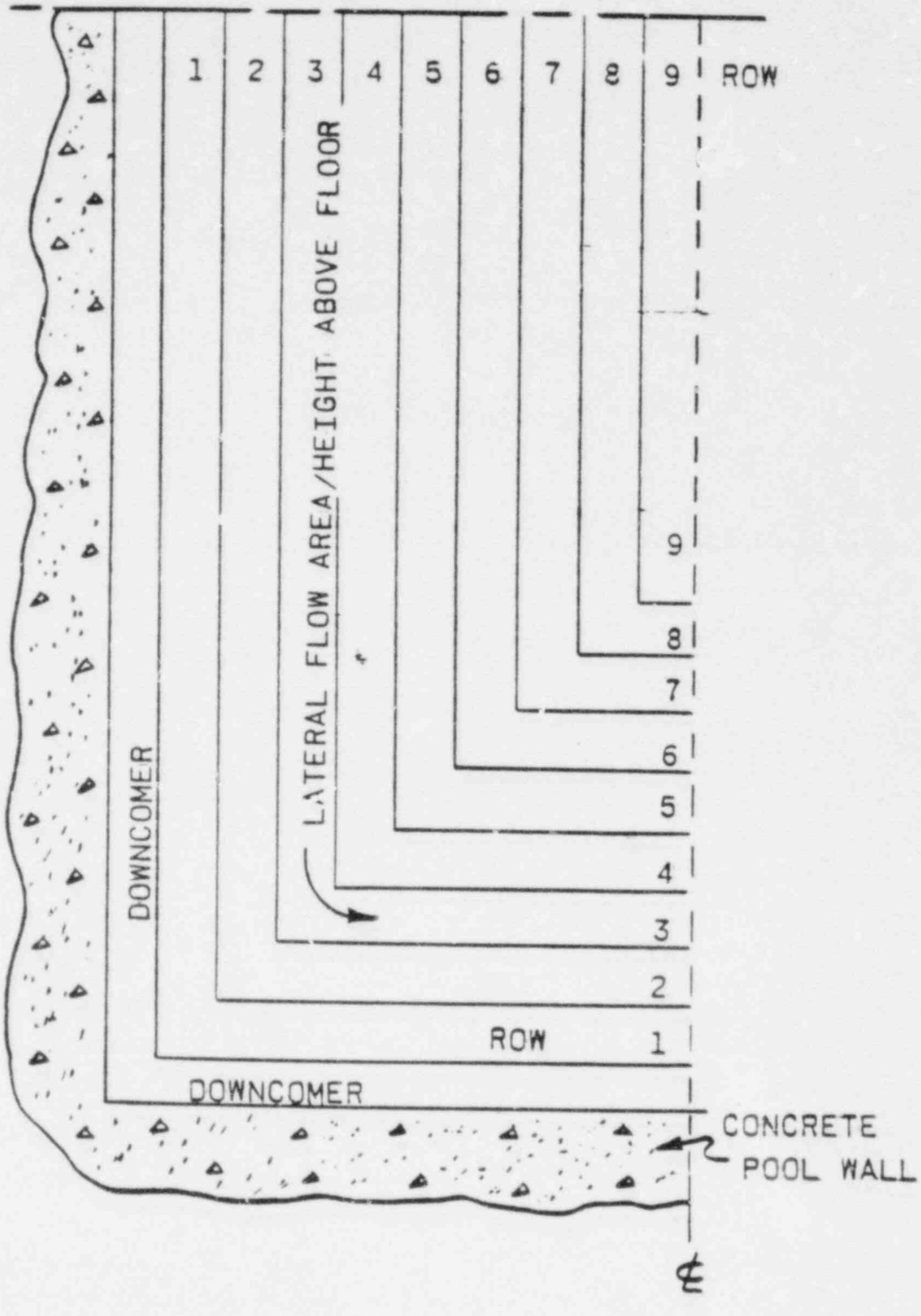

FIGURE 4-2
SPENT FUEL POOL NATURAL CIRCULATION MODEL
(PLAN VIEW)

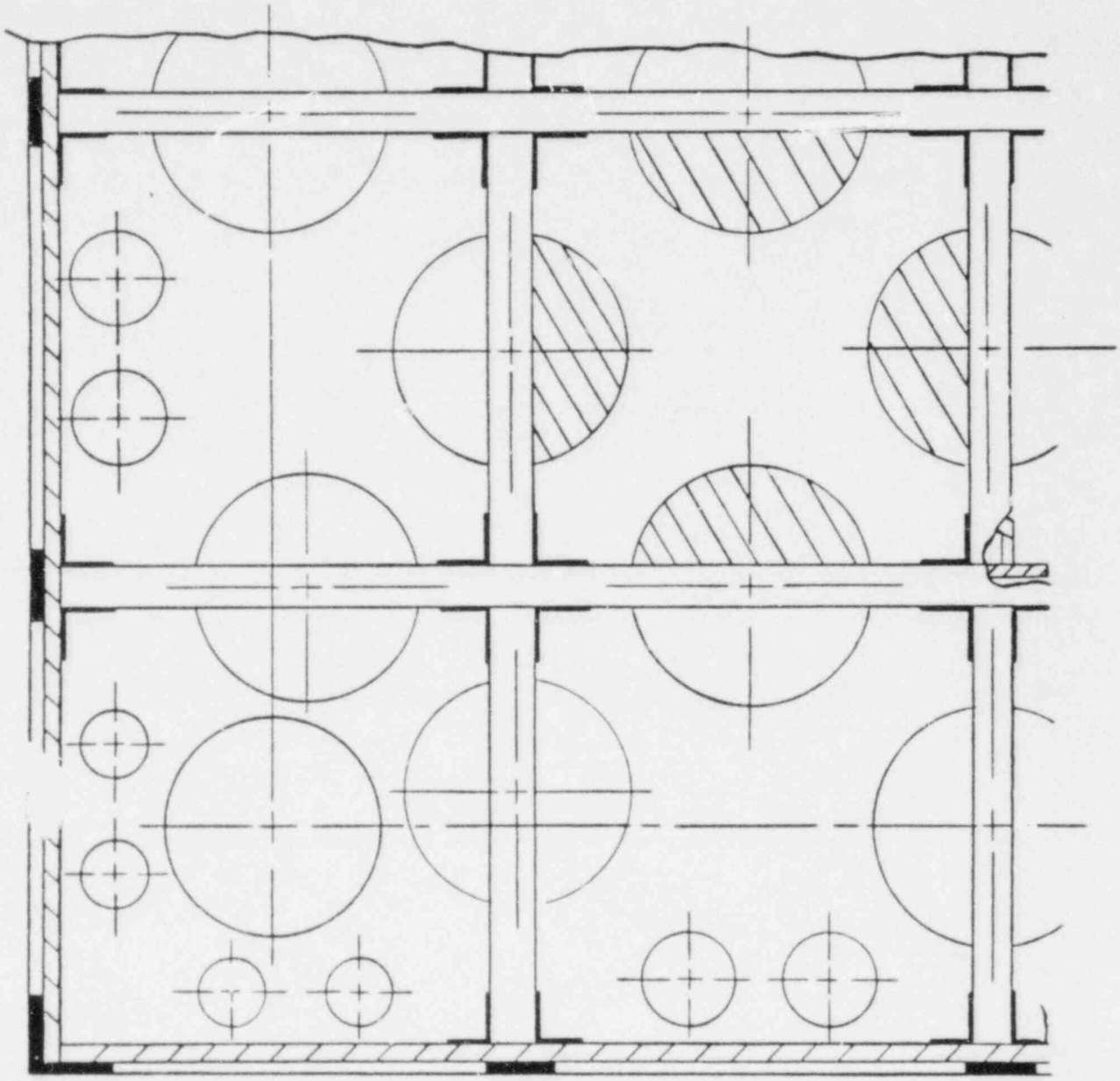

FIGURE 4-3

SPENT FUEL RACK INLET FLOW AREAS

The analyses that have been described only address the flow through the storage cells. As noted in the discussion of criteria, it is also required that the flow and temperatures in the axial gap between adjacent storage cells be evaluated. In order to preclude the possibility of stagnant conditions in these gaps, flow relief areas are provided at the location of the grid support structures as shown in Figure 4-4. This flow area also ensures that air or steam cannot be trapped in the rack structure as required by Reference 8. The thermal hydraulic conditions in the gap region are evaluated by using a parallel path thermal-hydraulic model of the gap and cell under consideration. This analysis considers the gamma heat generation in the cell enclosure, poison material and cell wrapper in addition to the decay heat input. Using the cell flow velocity and driving pressure differential obtained from the previously described pool analyses, the flow velocity in the gap and the axial temperature distributions of the coolant and structure are determined. The radial temperature distributions through the various components are also considered. Based on the magnitude of the flow through these gaps, the pool analysis may or may not be repeated using an appropriate increase in the total circulating flow in order to achieve a more conservative analysis. Generally, the gap analysis indicates that the pool temperature analysis is conservative since that analysis assumes no radial conduction out of the storage cell.

4.4 RESULTS

Three modes of operation were considered:

a. Normal Refueling

For this case, the analysis is based on a discharge of 68 fuel assemblies having an irradiation time of 1044 E.F.P.D. at a time equal to 150 hours after shutdown. The entire pool is filled with fuel discharged at one year intervals except for 205 locations that are reserved for the full core off-load.

FIGURE 4-4

INTERCELL FLOW AREA REGION

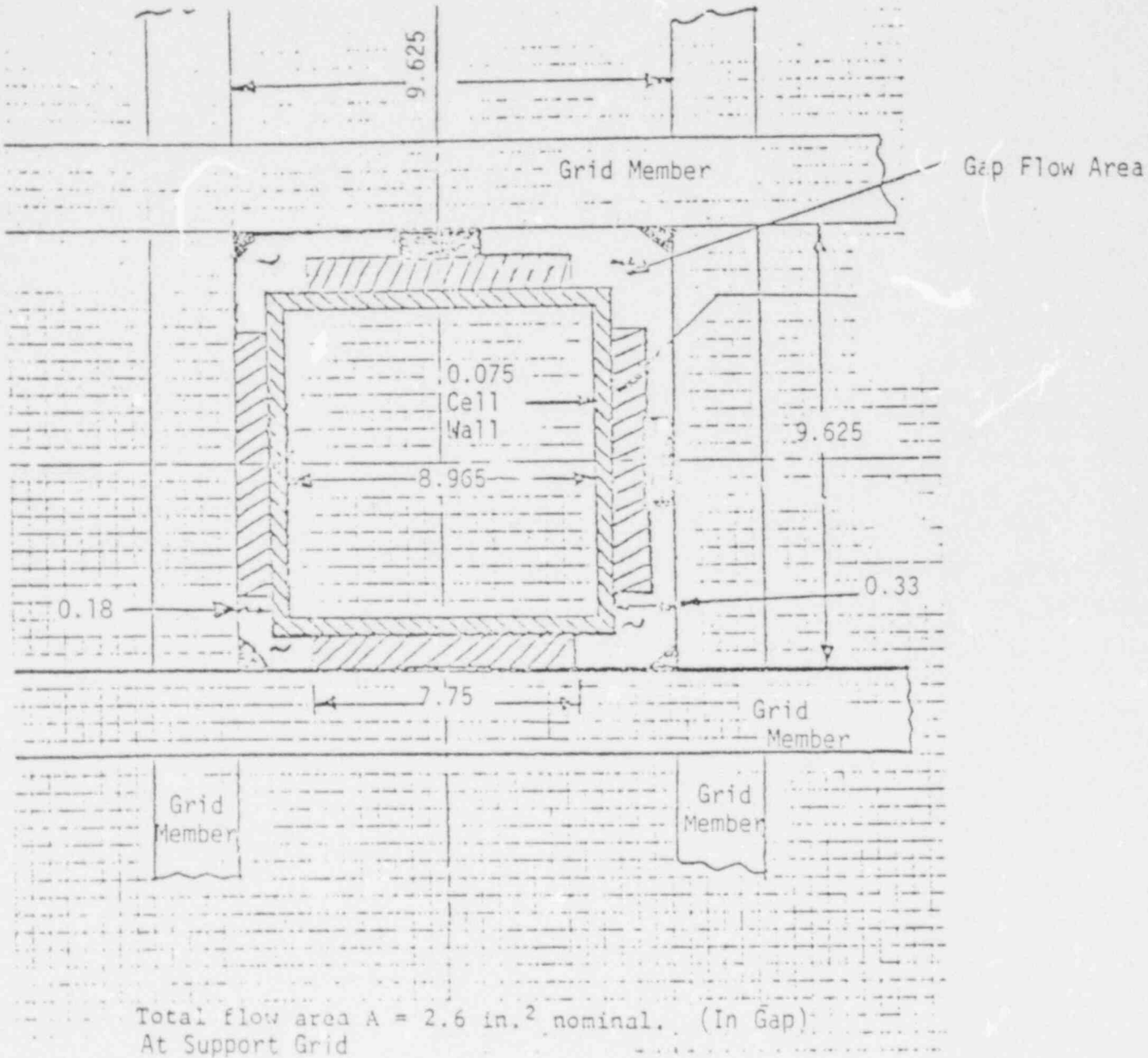

Total flow area A = 2.6 in.^{2} nominal. (In Gap)
At Support Grid

b. Special ore Off-Load

It is assumed that a full core of fuel is placed into the pool at 60 days following a normal refueling. This results in all storage cells being filled. It is further assumed that both spent fuel pool coolers and both pumps are operational. The cooling water flow to each cooler is reduced to the level specified in Table 9.1.3-1 of the Bellefonte SAR.

c. Abnormal Core Off-Load

This case is similar to the special core off-load except that only one spent fuel pool cooler and pump is operational.

4.4.1 Cell Outlet and Clad Surface Temperatures

The previously described method was used to evaluate the natural circulation velocities, coolant temperatures, and fuel rod cladding temperatures throughout the spent fuel pool for the three operating conditions. A brief summary of the results for the "hottest" cell follows:

Condition	Worst Cell Outlet Temperature	Maximum Clad Temperature	
		Average Rod	Peak Rod
Normal Refueling	171.8°	191.0°	202.0°
Special Core Off-Load	177.7°	194.5°	204.0°
Abnormal Core Off-Load	214.3°	230.5°	239.8°

Conclusions for the "hottest" cell analysis are:

a. Since the saturation temperature at the cell outlet is 240°, there is no bulk boiling for any of the cases.

b. The only case for which local subcooled boiling might be expected is the abnormal core off-load and even for that case, a peak to average rod heat flux of greater than 1.6 would be required.

4.4.2 Impact of Gamma Heating in BORAL on Water Between Adjacent Cells

The volumetric heat generation in the wall and wrapper, which are stainless steel, is in fact larger than the volumetric heat generation in the Boral. Note that at 100 hours after shutdown, the heating rate in the stainless is $1x10^4$ BTU/hr./ft.^{3} and in the Boral is $0.3x10^4$ BTU/hr./ft.^{3}. However, based on the volumes of the two materials, the total heat generation in the wall is roughly $5x10^3$ BTU/hr. which is less than 3 percent of the heat which is generated due to the stored fuel ($228x10^3$ BTU/hr.). Nevertheless, because of the possibility of low flow rates in the inter-cell gaps, an analysis was performed in order to evaluate the coolant and cell temperature distribution in these gaps. Since the heat generated in the cell is so small compared to that due to the fuel, the flow velocities through the cell that were obtained from the previous analyses were used for the inside of the cell and the flow in the gap was calculated based on the equality of pressure drops for the flow inside and outside of the cell.

Since the velocity in the gap between cells is also affected by the change in the density of flow, a thermal analysis which determined how much heat flowed to either side of the cell wall was coupled with the hydraulic analysis. This analysis also yielded the temperature distribution through the cell wall, the Boral plate, and the cell wrapper as a function of axial position. Because of the low flow velocities that were anticipated in the gaps, the model also has the capability of determining heat transfer coefficients for both laminar and turbulent; free and forced convection. The temperature of the flow entering the gap is assumed to be equal to that of the flow entering the cell since they are both fed by the laterial flow near the bottom of the pool. An iterative solution is then used to determine the axial temperature distribution and the flow velocity in the gap.

The analysis was performed for the three operating conditions which were previously identified: Normal refueling, special core off-load, and abnormal core off-load.

One of the key parameters in this evaluation is the minimum local flow area in the inter-cell gap. Based on Figure 4-4, the nominal value of the minimum flow area is 2.6 in. and the minimum value is 1.8 $in.^2$. The resulting maximum water temperatures are shown in the table below. These results confirm that the temperature of the water between the cells is less than that of the water in the cells and boiling is no concern even if the water level is allowed to reach its minimum value of 10 feet above the racks.

Condition	Local Minimum Flow Area (at Grid)	Maximum Cell Outlet Water Temperature	Maximum Gap Outlet Water Temperature
Normal Refueling	2.6 $in.^2$	171.8°	158.3°
	1.8 $in.^2$	171.8°	158.6°
Special Core Off-Load	2.6 $in.^2$	177.7°	166.5°
	1.8 $in.^2$	177.7°	166.8°
Abnormal Core Off-Load	2.6 $in.^2$	214.3°[1]	203.7°
	1.8 $in.^2$	214.3°[1]	204.0°

[1] Note that the saturation temperature with the nominal water head is 240° and with a 10 foot water head is 227°, so boiling is not a concern.

4.4.3 Conditions Following a Loss of Pool Cooling

Following a postulated failure of all of the external pool cooling systems, the temperature of the water in the pool rises at a rate which is determined by the quantity and age of the stored fuel as well as by the total volume of water in the pool at the time of failure. It is assumed in the natural circulation analysis that the pool surface temperature has already risen to the saturation temperature at atmospheric conditions (212°) and that all storage cells are filled. The pool water level is assumed to be maintained by the addition of water at a rate which equals the rate at which evaporation occurs.

The results show that the maximum storage cell outlet temperature is less than 230° and the maximum fuel clad surface temperature is less than 253° for this condition. Since the saturation temperature with the nominal water head is 240°, there is no boiling in the cell or inter-cell gaps.

5. STRUCTURAL AND SEISMIC CONSIDERATIONS

5.1 COMPONENT DESCRIPTION

The purpose of the structural analysis is to analyze the critical components/load paths under various loading conditions. Figure 5-1 shows the general arrangement of a typical fuel rack assembly and its attachment to the pool.

The complete fuel rack assembly is divided into four major sections for stress analysis purposes as follows:

a. Embedment connection assembly

b. Leveling pad assembly

c. Lower and upper grid assembly

d. Cell assembly

The following paragraphs describe each assembly.

5.1.1 Embedment Connection Assembly

The adapter plate is attached to the spent fuel pool by using a 2-8 UN threaded stud. The stud is welded to a one inch stainless steel plate, which is welded to the leak chase channel system and set in grout. The main function of the stud is to connect the adapter plate to the spent fuel pool embedment, thus preventing the free sliding of the adapter plate during a horizontal seismic event. The stud is seal welded to the one inch plate under the pool liner to prevent any leakage of the spent fuel pool coolant water. The seal weld is designed to withstand the maximum horizontal load. A shear pin is shrunk fit into the adapter plate and provides the means for transferring horizontal loads between the racks and the adapter plates.

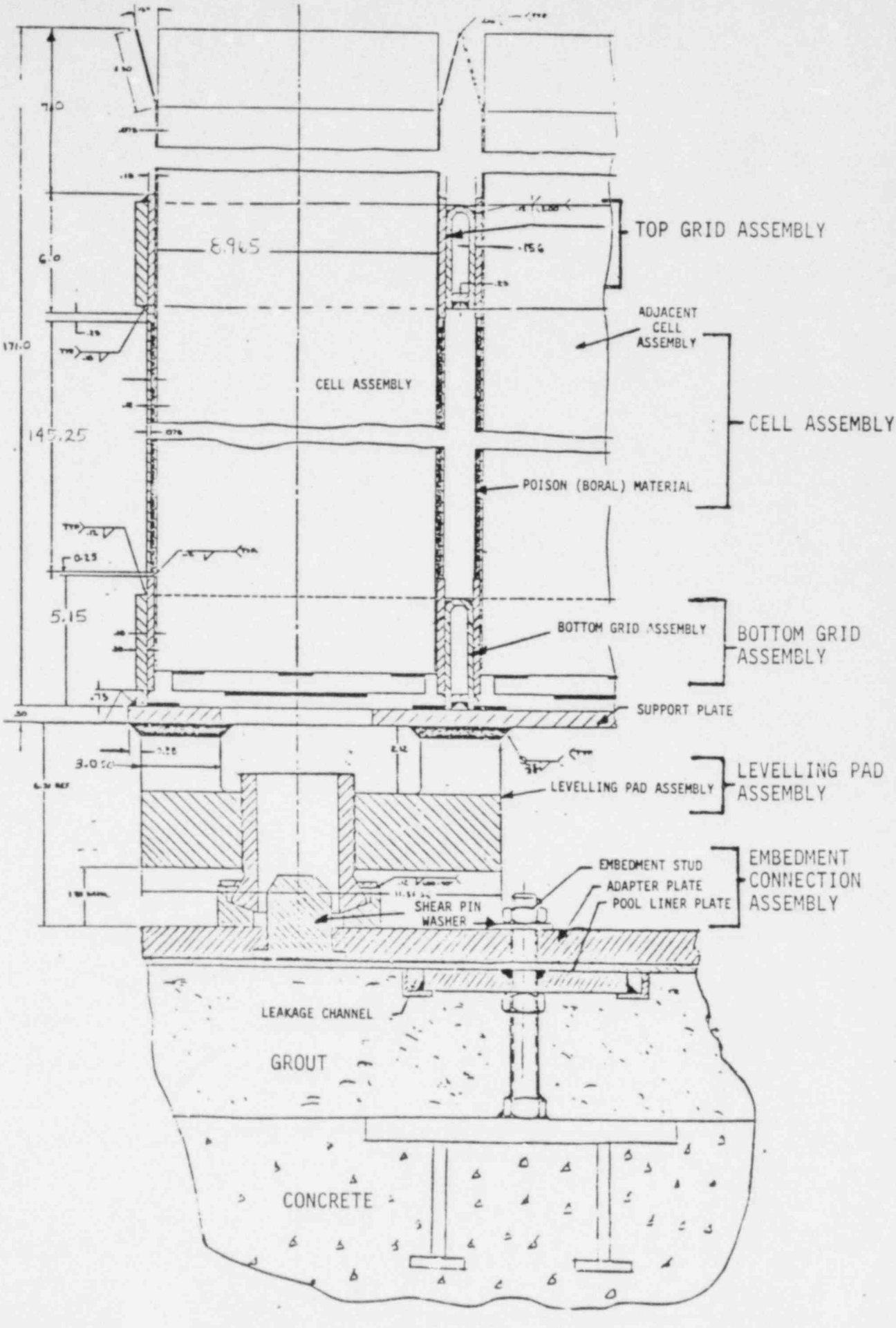

FIGURE 5-1

FUEL RACK ASSEMBLY

5.1.2 Leveling Pad Assembly

The top end of the leveling pad assembly is welded to the support plate. The bottom end locates around the shear pins of the adapter plates. During the horizontal seismic event, the shear pin resists the horizontal load and prevents the sliding of the rack. There are ten leveling pad assemblies for each rack assembly. The leveling pad screw permits the leveling adjustment of the rack. The major components of the leveling pad assembly are the leveling pad, the leveling pad screw, and the shear pin.

5.1.3 Lower and Upper Grid Assembly

The lower grid attaches the cell assembly to the support plate. The lower grid consists of U-beam members, the spacer plates and the support plate. The cell assembly at bottom is welded to the lower grid through the spacer plate. The upper grid consists of the U-beam members and the spacer plates. The cell assembly at the top is welded to the upper grid through the spacer plate. The upper and lower grid assembly maintains the precise center-line to center-line spacing between the cells and provides the structural connections between the cells to form a fuel rack assembly.

5.1.4 Cell Assembly

The major components of the cell assembly are the fuel assembly cell, the Boral (neutron absorbing) material, the wrapper, and the upper and lower spacer plates.

The ID of the cell is 8.965 with a 0.075 inch wall. The upper end of the cell has a funnel shape flare for easy insertion of the fuel assembly. The wrapper is attached to the outside of the cell through a seam welding along the entire length of the wrapper. Thus, the wrapper forms an encapsulation for the Boral material. The top and bottom spacer plates are welded to the upper and lower grid assembly. thus providing a structural connection between the cell and the grid assembly.

Depending upon the criticality requi. ments, some cells have a Boral encapsulation on all four sides, some on three sides, and some on two sides. The spacer plate seal-weld is a continuous weld when it is to provide a leak-tight encapsulation. However, when the spacer plate is welded to a cell side that has no Boral encapsulation, an intermittent weld is used.

5.2 DESIGN AND ANALYSIS PROCEDURES

5.2.1 Seismic Analysis Models

The dynamic response of the fuel rack assembly during a seismic event is the condition which produces the governing loads and stresses on the structure. The dynamic response and internal stresses and loads are obtained from a seismic analysis which is performed in two phases. The first phase is a time history analysis on a single cell nonlinear finite element model. The second phase is a response spectrum analysis of a detail rack assembly finite element model. The damping values used in the seismic analysis are two percent damping for OBE and four percent damping for SSE.

The single cell nonlinear model has the structural characteristics of an individual cell within a submerged rack assembly. The nonlinearities of the model account for the effects of the gap between the fuel cell and the fuel during seismic excitation. The MODAL superposition method in the WECAN computer program was used to determine the time history response of the fuel assembly/fuel rack system. The theory of the MODAL superposition method in WECAN is given in WCAP-9389. The effective fuel mass, fuel assembly to cell impact loads, and overall rack response are obtained from the nonlinear time history response of this model. In determining the maximum response for each item of interest, the response value for each item was searched for maximum values.

The detail model is a three-dimensional finite element representation of an 11 x 12 rack assembly consisting of discrete three-dimensional beams

interconnected at a finite number of nodal points. The 11 x 12 rack assembly was used because the seismic response is greater for the 11 x 12 rack in the 11 cell direction than that of the 12 x 12 rack. The frequency of the rack in the 11 cell direction is less than that in the 12 cell direction, thus providing higher acceleration values from the response spectrum. The closer spaced support points on the 11 x 12 rack produce higher loads on the support pad in the 11 cell direction.

The results of the nonlinear time history model are incorporated in the detail model. Since the detail model does not account for the nonlinear effect of a fuel assembly impacting the cell and the hydrodynamic restoring force, the internal loads and stresses for the rack assembly obtained from this model are corrected by load correction factors. The load correction factor is derived from the single cell nonlinear model results and is applied to the components in the Structural Analysis, Section 5.2.2. The responses of the model from accelerations in three directions are combined by the SRSS method in the structural analysis. The loads in four major components (support pad assembly, bottom grid, top grid, and fuel cell) are examined, and the maximum loaded section of each of these components is found. These maximum loads from the detail model are used in the structural analysis to obtain the stresses within the rack assembly.

5.2.2 Structural Analysis

5.2.2.1 Loads and Load Combinations

The loads and load combinations to be considered are those given in NRC Standard Review Plan, Section 3.8.4-II.3. The thermal loads due to rack expansion relative to the pool floor are negligible since the shear pins and embedment studs are provided. The major seismic loads are produced by the operational basis earthquake (OBE) and safe shutdown earthquake (SSE) events.

It is noted from the seismic analysis that the magnitude of stresses vary considerably from one geometrical location to the other in the model. Consequently, the maximum loaded cell assembly, grid assembly and the leveling pad assembly are analyzed. Such an analysis envelopes the other areas of the rack assembly.

Because of structural symmetry of the cell assembly about the x and y axes, the x and y direction horizontal seismic events produce identical loads. Consequently, the margins of safety for the multi-direction (x and y directions simultaneously) seismic event is computed by multiplying the unidirectional loads by $\sqrt{2}$.

The grid assembly margins of safety for the multi-direction seismic event are produced by combining x-direction and y-direction loads by SRSS.

The margins of safety, due to the multi-direction shock for the leveling pad assembly, are the same as the uni-direction because maximum stresses, due to x-direction and y-direction seismic acceleration, do not occur at the same point. The multi-direction seismic event stresses for the weld of the leveling pad assembly are properly corrected.

The loads described in the seismic analysis section are corrected by load correction factor of 0.35 for the moments and 0.66 for the forces.

5.2.2.2 Fuel Handling Crane Uplift Analysis

The objective of this analysis is to ensure that the rack can withstand a maximum uplift load of 4500 pounds of the fuel handling crane without violating the criticality acceptance criteria.

Two accident loading conditions are postulated. The first condition assumes that the uplift load is applied to a fuel cell. The second

condition assumes that the load is applied to the top grid. Calculations show that for either condition, the resulting stresses are within acceptable stress limits. There is no change in rack geometry and the criticality acceptance criteria is not violated.

5.2.2.3 Fuel Assembly Drop Accident Analysis

The objectives of this analysis are to ensure that, in the unlikely event of dropping a fuel assembly, accidental deformation to the rack will not cause the criticality acceptance criteria to be violated, and the spent fuel pool liner will not be perforated.

Two accident conditions are postulated. The first accident condition assumes that a fuel assembly impacts on the top of the rack. Calculations show that the impact energy is absorbed by the cell funnels and the section of cell above the upper grid which undergo deformation. If in the unlikely event that two adjacent cells are crushed together for their full length, criticality calculations show that $K_{eff} <$ 0.95. Under these faulted conditions, credit is taken for dissolved boron in the water, and the criticality acceptance criteria is not violated for the Bellefonte poison spent fuel racks. The spacing between the cells and the racks is such that pool liner performation is not a concern in this accident condition.

The second accident condition assumes that the fuel assembly falls straight through an empty cell, and impacts the rack base plate from a drop height of 222 inches. The results of this analysis show that the impact energy is absorbed by the guide thimbles, bottom nozzle legs, and the rack base plate. The spent fuel pool liner will not be perforated and the margin of safety is 0.156. Criticality calculations show that $K_{eff} < 0.95$ and the criticality acceptance criteria is not violated for the Bellefonte poison spent fuel racks.

In both these accident conditions, the criticality acceptance criteria is not violated and the spent fuel pool liner is not perforated.

5.2.2.4 Structural Acceptance Criteria

The fuel racks are analyzed for the normal and faulted load combinations of Section 2.2 in accordance with the "NRC Position for Review and Acceptance of Spent Fuel Storage and Handling Applications."

The major normal and upset condition loads are produced by the operational basis earthquakes (OBE). The thermal stresses due to rack expansion relative to the pool floor are negligible since sufficient clearances between the rack leveling pads and the adapter plate shear pins are provided.

The faulted condition loads are produced by the safe shutdown earthquakes (SSE) and a postulated fuel assembly drop accident.

The computed stresses are below the allowable stresses as required by the ASME B+PV Code, Section III, Subsection NF.

In summary, the results of the seismic and structural analysis show that the Bellefonte spent fuel storage racks meet all the structural acceptance criteria adequately.

6. MATERIALS

6.1 ACCEPTANCE MATERIALS

Construction materials conform to the requirements of ASME Code, Section III, Subsection NF. All the materials used in the construction are compatible with the storage pool environment and do not contaminate the fuel assemblies or the pool water. The racks are constructed from type 304 stainless steel. Material properties for the rack components are shown in the following table.

TABLE OF MATERIAL PROPERTIES

MATERIAL	Temperature, T		
	75°F	110°	150°
SA240 and SA479 Type 304			
S_u, Ksi	75.0	74.6	73.0
S_y, Ksi	30.0	29.5	27.5
S_m, Ksi	20.0	20.0	20.0
E, $x10^{+6}$ psi	28.3	28.1	27.93
α, 10^{-6} psi	9.11	9.17	9.25

6.2 NEUTRON ABSORBING MATERIAL

The neutron absorbing material, Boral, used in the Bellefonte spent fuel rack construction is produced by Brooks and Perkins, Inc. The Boral plates have a minimum 10B areal density of 0.02 gm/cm^2. The Boral material is sealed from the pool environment and the cells containing Boral are leak tested.

7. FABRICATION AND QUALITY CONTROL

The Bellefonte spent fuel rack components and assemblies are fabricated in accordance with the "NRC" Position on Review and Acceptance of Spent Fuel Storage and Handling Applications" and meet the Quality Assurance Program requirements of WCAP-8370.

8. CONSLUSION

This report has examined the design and safety aspects of the Bellefonte poison spent fuel storage racks in the following areas:

a. Nuclear Criticality
b. Thermal-Hydraulic
c. Structural and Seismic
d. Materials

In these areas, the racks are designed in accordance with "NRC" Position for Review Acceptance of Spent Fuel Storage and Handling Applications," and adequately meet the requirements of the applicable codes and standards.

REFERENCES

1. W. E. Ford III, et al, "A 218-Group Neutron Cross-Section Library in the AMPX Master Interface Format for Criticality Safety Studies," ORNL/CSD/TM-4 (July 1976).

2. N. M. Greene, et al, "AMPX: A modular Code System for Generating Coupled Multigroup Neutron-Gamma Libraries from ENDF/B," ORNL/TM-3706 (March 1976).

3. L. M. Petrie and N. F. Cross, "KENO IV--An Improved Monte Carlo Criticality Program," ORNL-4938 (November 1975).

4. S. R. Bierman, et al, "Critical Separation Between Subcritical Clusters of 2.35 wt percent ^{235}U Enriched UO_2 Rods in Water with Fixed Neutron Poisons," Battelle Pacific Northwest Laboratories PNL-2438 (October 1977).

5. S. R. Bierman, et al, "Critical Separation Between Subcritical Clusters of 4.29 wt percent ^{235}U Enriched UO_2 Rods in Water with Fixed Neutron Poisons," Battelle Pacific Northwest Laboratories PNL-2615 (March 1978).

6. J. T. Thomas, "Critical Three-Dimensional Arrays of U (93.2) -- Metal Cylinders," Nuclear Science and Engineering, Volume 52, pages 350-359 (1973).

7. Specification for the Design, Fabrication, and Delivery of Poison Spent Fuel Storage Racks. TVA Specification Number 79K67-824481, dated 8/30/79.

8. NRC Position for Review and Acceptance of Spent Fuel Storage and Handling Applications dated 4/14/78 and Modifications dated 1/18/79.

9. NRC Standard Review Plan 9.1.3.

10. Design Objectives for Light Water Spent Fuel Storage Facilities at Nuclear Power Plants ANSI-N210.

DOCUMENT/ PAGE PULLED

ANO. 8107290265

NO. OF PAGES 1

REASON

☐ PAGE ILLEGIBLE

☐ HARD COPY FILED AT: PDR CF

OTHER _____

☐ BETTER COPY REQUESTED ON ____/____/____

☒ PAGE TOO LARGE TO FILM

☒ HARD COPY FILED AT: (PDR) CF

OTHER _____

☒ FILMED ON APERTURE CARD NO 8107290265 - 01